

Periodic Sources of Gravitational Waves

Luciano Rezzolla*

SISSA, International School for Advanced Studies and INFN, Trieste, Italy

Department of Physics and Astronomy, Louisiana State University, Baton Rouge, LA 70803 USA

Lectures given at the Villa Mondragone International School of Gravitation and Cosmology:

“Looking for a needle in a haystack: how to extract a GW signal from the detectors data”, Sept. 7th – 10th, 2004 Frascati (Rome), Italy

*www.sissa.it/~rezzolla

1 Periodic Sources: some definitions

In principle, periodic sources of gravitational radiation are at those producing gravitational waves of amplitude

$$h_+(t) = \sum_j (h_{0+})_j \cos(2\pi f_j t + \phi_j), \quad h_\times(t) = \sum_j (h_{0\times})_j \sin(2\pi f_j t + \phi_j), \quad (1)$$

where $(h_{0+})_j, (h_{0\times})_j$ are the (constant) wave-amplitudes in the two polarization states at the frequencies f_j , while ϕ_j are constant phases. For simplicity we will consider the simpler case in which the source is emitting gravitational wave at a single frequency f .

Given a detector whose response has a power spectral density $S_h(f)$ and a strain noise $h_n(f) = \sqrt{f S_h(f)}$, the signal-to-noise ratio will be given by

$$\frac{S}{N} \simeq \frac{h_c}{h_n(f)} \langle [F_+(r, \theta, \phi, \psi)]^2 \rangle^{1/2} \simeq \frac{1}{\sqrt{5}} \frac{h_c}{h_n(f)}, \quad (2)$$

where $F_+(r, \theta, \phi, \psi)$ is beam pattern function of the detector (ψ is the polarization angle),

$\langle \dots \rangle$ indicates a time average and h_c is the *characteristic frequency* of the signal

$$h_c \equiv \sqrt{\frac{2}{3}} \langle [h_{0+}(i, r)]^2 + [h_{0\times}(i, r)] \rangle^{1/2}. \quad (3)$$

where i is the inclination angle.

In practice, periodic sources do not exist. However, they can be considered as such on timescales which are much shorter than the timescale over which the emission period changes. A good example in this respect is offered by the electromagnetic waves emitted by pulsar which are not perfectly periodic but that have a typical rate of change in the period of the order: $P_{\text{rot}} \dot{P}_{\text{rot}} \simeq 10^{-15} B_{12}^2 \text{ sec}$.

Periodic sources in general are very attractive since they allow for a simple modelization and for long integration times over which stochastic fluctuations are averaged out. There are several sources of gravitational radiation that could be, at some stage in their evolution,

effectively periodic and among these are

1. rotating neutron stars
2. rotating neutron stars deformed by crystalline or magnetic stresses
3. oscillating neutron stars
4. dynamical and secular non-axisymmetric instabilities
5. binary neutron stars

I will give a very brief overview of points 1. – 4., although further details on 3. and 5. will be also given by other lecturers in this school.

2 Rotating Neutron Stars

A rotating neutron star, such as a pulsar, will emit periodic gravitational waves as a result of small deviations from symmetry around its rotation axis. Such gravitational waves will be in general at several different frequencies, with an amplitude that will depend on how large these deviations are and on how rapid the star rotates. Note that, at least in principle, a rotating neutron star can emit gravitational waves also if it remains perfectly axisymmetric so long as it has a time varying mass quadrupole; the gravitational waves in this case will carry away energy but not angular momentum. We will not consider this case hereafter.

Typical neutron stars have masses $M \simeq 1.4M_{\odot}$ and radii $R \simeq 10$ km, which makes them among the most relativistic astrophysical objects (i.e. $M/R \simeq 0.2$). On the

other hand, typical neutron stars have rotation periods $P_{\text{rot}} \gtrsim 1 - 3$ msec and produce the most intense gravitational waves at frequencies $f = 2/P_{\text{rot}}$, with a corresponding reduced wavelength $\lambda/(2\pi) \gtrsim 30 - 70$ km. The *near-zone* will extend up $\lambda/(2\pi)$, where gravity will be of the order $2\pi M/\lambda \lesssim 0.03 \times (3 \text{ msec}/P_{\text{rot}})$ and sufficiently weak so that a nearly Lorentzian coordinate system can be chosen there. I will refer to this reference frame as the *asymptotic inertial frame* and will introduce a set of spatial basis vectors $\mathbf{e}_x, \mathbf{e}_y, \mathbf{e}_z$.

If the star is rotating with angular velocity Ω_{rot} , it will be flattened by centrifugal forces and may also deviate from axisymmetry as a result of shear forces produced either by crystalline or magnetic stresses. Because of this, it is useful to introduce a reference frame, the *asymptotic corotating frame* whose spatial basis vectors $\mathbf{e}_{x'}, \mathbf{e}_{y'}, \mathbf{e}_{z'}$ are along the principal

axes of the star (cf. Fig. 1), so that the quadrupole moment in this frame will take the form

$$\mathbf{I} \equiv \varepsilon_p I [\mathbf{e}_{z'} \otimes \mathbf{e}_{z'} - \frac{1}{2}(\mathbf{e}_{x'} \otimes \mathbf{e}_{x'} + \mathbf{e}_{y'} \otimes \mathbf{e}_{y'})] + \frac{1}{2} \varepsilon_e I (\mathbf{e}_{x'} \otimes \mathbf{e}_{x'} - \mathbf{e}_{y'} \otimes \mathbf{e}_{y'}), \quad (4)$$

where ε_p is the stellar *poloidal gravitational oblateness* and ε_e the stellar *equatorial gravitational oblateness*, defined respectively as

$$\varepsilon_p I \equiv \mathcal{I}_{z'z'}, \quad \varepsilon_e I \equiv \mathcal{I}_{x'x'} - \mathcal{I}_{y'y'}, \quad (5)$$

where, in general, $\varepsilon_e \ll \varepsilon_p \ll 1$. Clearly, as the star rotates, it will carry the basis vectors of its corotating frame around with itself at a rate which is given by the standard transformation rule for rotating frames

$$\frac{d\mathbf{e}_{j'}}{dt} = \boldsymbol{\Omega}_{\text{rot}} \times \mathbf{e}_{j'}. \quad (6)$$

Furthermore, the star, just like the earth or the sun, is also likely to precess with angular

velocity $\Omega_{\text{prec}} = \Omega_{\text{prec}} \mathbf{e}_{z'}$, so that the *total angular velocity* will be

$$\boldsymbol{\Omega} = \boldsymbol{\Omega}_{\text{rot}} + \boldsymbol{\Omega}_{\text{prec}}, \quad \text{and} \quad \boldsymbol{\Omega} = \Omega \mathbf{e}_z. \quad (7)$$

is a constant of motion in the asymptotic inertial frame.

As seen in the corotating frame, the angular velocity of rotation $\boldsymbol{\Omega}_{\text{rot}}$ will precess at a constant rate Ω_{prec} around the near axisymmetry axis $\mathbf{e}_{z'}$

$$\frac{d\boldsymbol{\Omega}_{\text{rot}}}{dt} = \boldsymbol{\Omega}_{\text{prec}} \times \boldsymbol{\Omega}_{\text{rot}}, \quad (8)$$

keeping the angle to that that axis $\theta_w \equiv \cos^{-1}(\boldsymbol{\Omega}_{\text{rot}} \cdot \mathbf{e}_{z'}) = \text{const.}$ constant in time. The angle θ_w is referred to as the “*wobble angle*” and, because $\boldsymbol{\Omega} = \text{const.}$, the rate of change of the precession angular velocity is the same as that of the angular velocity

$$\frac{d\boldsymbol{\Omega}_{\text{prec}}}{dt} = \Omega_{\text{prec}} \frac{d\mathbf{e}_{z'}}{dt} = \boldsymbol{\Omega}_{\text{rot}} \times \boldsymbol{\Omega}_{\text{prec}} = -\frac{d\boldsymbol{\Omega}_{\text{rot}}}{dt}. \quad (9)$$

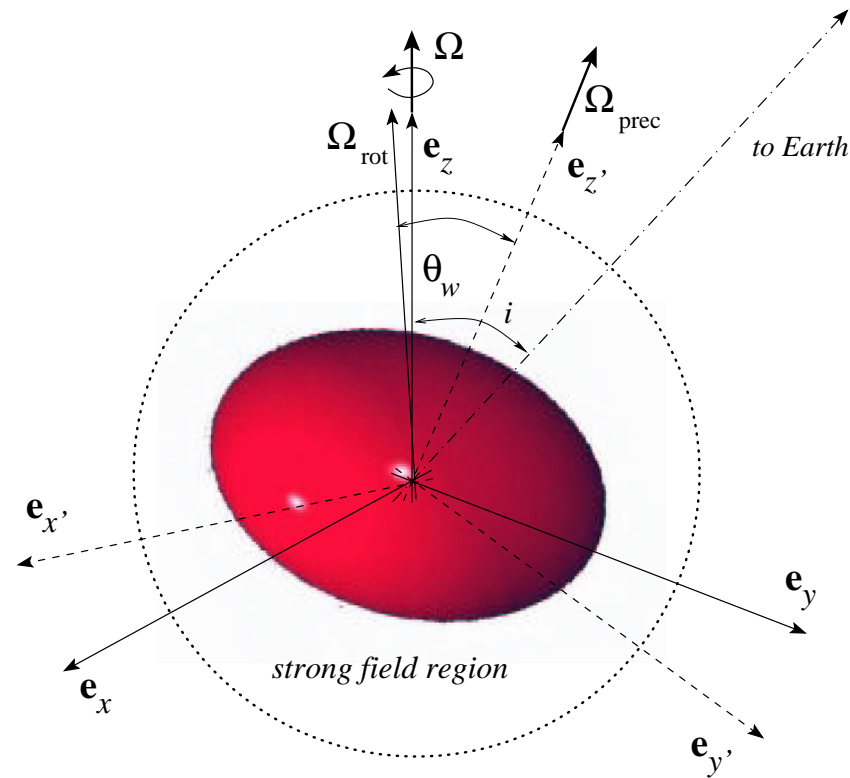


Figure 1: Schematic view of a rotating neutron star and of the relevant reference frames: the *asymptotic inertial frame* (basis vectors e_i) and the *asymptotic corotating frame* (basis vectors $e_{i'}$). Note that in general $\Omega = \Omega_{\text{rot}} + \Omega_{\text{prec}}$, although in practice $\Omega \approx \Omega_{\text{rot}}$.

A schematic description of the two asymptotic frames is shown in Fig. 1 where are indicated the different orientations of angular velocity vectors Ω , Ω_{rot} , and Ω_{prec} .

Note that because of the large degree of axisymmetry expected in neutron stars, the wobble angle is in general very small $\theta_w \ll 1$ and that since $\boldsymbol{\Omega} = \boldsymbol{\Omega}_{\text{rot}} + \boldsymbol{\Omega}_{\text{prec}}$, not $\boldsymbol{\Omega}_{\text{rot}}$, nor $\boldsymbol{\Omega}_{\text{prec}}$ will be aligned with \mathbf{e}_z and that small angles will exist between these three vectors.

In particular, since

$$\frac{\theta_0}{\theta_w} = \frac{(\text{angle between } \boldsymbol{\Omega}_{\text{rot}} \text{ and } \mathbf{e}_z)}{(\text{angle between } \boldsymbol{\Omega}_{\text{rot}} \text{ and } \mathbf{e}_{z'})} = \frac{\Omega_{\text{prec}}}{\Omega_{\text{rot}}} \sim 10^{-5} - 10^{-8} \ll 1. \quad (10)$$

So far we have concentrated on the dynamics of the system but it is time to consider its gravitational wave emission. Within a Newtonian quadrupole approximation (the one we will assume hereafter¹), the gravitational wave emission can be calculated by computing the time variations of the stellar mass quadrupole defined as

$$\mathcal{I}_{jk} \equiv \int \rho(x^j x^k - \frac{1}{3} r^2 \delta_{jk}) d^3x = -I_{jk} + \frac{1}{3} I_i^i \delta_{jk}, \quad (11)$$

¹Clearly, this is an approximation but given the uncertainties in the stellar structure and thus in the calculations of the mass quadrupole, it is not the worse one.

where I_{jk} is the stellar moment of inertia.

$$I_{jk} \equiv \int \rho(r^2 \delta_{jk} - x^j x^k) d^3x. \quad (12)$$

The problem is therefore quite simple: given the asymptotic inertial frame (the one in which the detector is placed), calculate (11) and its time variations. Since in the corotating frame the oblatenesses are readily defined as

$$\varepsilon_p = \frac{2I_{z'z'} - I_{x'x'} - I_{y'y'}}{I_{z'z'} + I_{x'x'} + I_{y'y'}}, \quad \varepsilon_e = \frac{3(I_{x'x'} - I_{y'y'})}{I_{z'z'} + I_{x'x'} + I_{y'y'}}, \quad (13)$$

we can use the expressions introduced above between the inertial and corotating inertial

frames, it is possible to calculate the changes of the latter to be

$$\mathbf{e}_{x'} = \cos(\Omega_{\text{rot}}t)\mathbf{e}_x + \sin(\Omega_{\text{rot}}t)\mathbf{e}_y + -\theta_w \cos(\Omega_{\text{prec}}t)\mathbf{e}_z, \quad (14)$$

$$\mathbf{e}_{y'} = -\sin(\Omega_{\text{rot}}t)\mathbf{e}_x + \cos(\Omega_{\text{rot}}t)\mathbf{e}_y + -\theta_w \sin(\Omega_{\text{prec}}t)\mathbf{e}_z, \quad (15)$$

$$\mathbf{e}_{z'} = \mathbf{e}_z + \theta_w \cos[(\Omega_{\text{rot}} + \Omega_{\text{prec}})t]\mathbf{e}_x + \theta_w \sin[(\Omega_{\text{rot}} + \Omega_{\text{prec}})t]\mathbf{e}_y, \quad (16)$$

$$(17)$$

so that the evolution of the quadrupole moment components are

$$\mathcal{F}_{xx} = -\frac{1}{2}\varepsilon_p I + \frac{1}{2}\varepsilon_e I \cos(2\Omega_{\text{rot}}t), \quad \mathcal{F}_{yy} = -\frac{1}{2}\varepsilon_p I - \frac{1}{2}\varepsilon_e I \cos(2\Omega_{\text{rot}}t), \quad (18)$$

$$\mathcal{F}_{zx} = 2\theta_w \varepsilon_p I \cos[(\Omega_{\text{rot}} + \Omega_{\text{prec}})t], \quad \mathcal{F}_{zy} = 2\theta_w \varepsilon_p I \sin[(\Omega_{\text{rot}} + \Omega_{\text{prec}})t], \quad (19)$$

$$\mathcal{F}_{zz} = \varepsilon_p I, \quad \mathcal{F}_{xy} = \frac{1}{2}\varepsilon_e I \sin(2\Omega_{\text{rot}}t). \quad (20)$$

Equations (18)–(20) show that the tensor components form two distinct classes that contain all of the relevant information on the gravitational waves and which can be summarized as follows

- *i)* the components of \mathcal{F}_{za} with $a = x, y$ change with frequency $\Omega_{\text{rot}} + \Omega_{\text{prec}}$;
- *ii)* the components of \mathcal{F}_{ab} with a and b equal to x, y change with frequency $2\Omega_{\text{rot}}$;

- *ii)* the two changes correspond to the rotation of the poloidal (cf. proportionality to ε_p and θ_w), and of the equatorial oblatenesses (cf. proportionality to ε_p), respectively;
- *iii)* the first change would be present even in the case of a perfectly axisymmetric star but the second one could contain important information on shear stresses and therefore on nuclear matter.

What will be observed at the detector? Let us suppose that the waves polarization axes are

$$\mathbf{e}_{\bar{x}} = \mathbf{e}_x, \quad \text{and} \quad \mathbf{e}_{\bar{y}} = \cos i \mathbf{e}_y - \sin i \mathbf{e}_z, \quad (21)$$

then the two polarizations will have amplitudes

$$h_+ = \frac{2}{r} \frac{d^2 \mathcal{F}_{\bar{x}\bar{x}}}{dt^2} = -\frac{2}{r} \frac{d^2 \mathcal{F}_{\bar{y}\bar{y}}}{dt^2}, \quad h_\times = \frac{2}{r} \frac{d^2 \mathcal{F}_{\bar{x}\bar{y}}}{dt^2}, \quad (22)$$

so that

$$h_+ = \frac{2(1 + \cos^2 i)}{r} \varepsilon_e I \Omega_{\text{rot}}^2 \cos(2\Omega_{\text{rot}} t) + \frac{2 \sin 2i}{r} \varepsilon_p I \theta_w \Omega_{\text{rot}}^2 \cos[(\Omega_{\text{rot}} + \Omega_{\text{prec}})t], \quad (23)$$

$$h_\times = \frac{4 \cos i}{r} \varepsilon_e I \Omega_{\text{rot}}^2 \sin(2\Omega_{\text{rot}} t) + \frac{4 \sin i}{r} \varepsilon_p I \theta_w \Omega_{\text{rot}}^2 \sin[(\Omega_{\text{rot}} + \Omega_{\text{prec}})t], \quad (24)$$

Note how expressions (23)–(24) clearly separate the contributions coming from the equatorial oblateness and oscillating at $2\Omega_{\text{rot}}$ from its sideband contribution coming from the poloidal oblateness and oscillating at $\Omega_{\text{rot}} + \Omega_{\text{prec}}$. Expressing now the amplitude in terms of the characteristic amplitudes we obtain

$$h_{c1} = 8\pi^2 \sqrt{\frac{2}{15}} \frac{\theta_w \varepsilon_p I (2f_1)^2}{r} \simeq 7.7 \times 10^{-20} \theta_w \varepsilon_p \left(\frac{I}{10^{45} \text{ g cm}^2} \right) \left(\frac{2f_1}{1 \text{ kHz}} \right)^2 \left(\frac{10 \text{ kpc}}{r} \right), \quad (25)$$

$$h_{c2} = 8\pi^2 \sqrt{\frac{2}{15}} \frac{\varepsilon_e I f_2^2}{r} \simeq 7.7 \times 10^{-20} \varepsilon_e \left(\frac{I}{10^{45} \text{ g cm}^2} \right) \left(\frac{f_2}{1 \text{ kHz}} \right)^2 \left(\frac{10 \text{ kpc}}{r} \right), \quad (26)$$

where $f_1 \equiv (\Omega_{\text{rot}} + \Omega_{\text{prec}})/2\pi$ and $f_2 \equiv \Omega_{\text{rot}}/\pi \simeq 2f_1$ is the high-frequency part of the signal.

Note how $h_c \propto \varepsilon_{\text{e,p}}$ and $h_c \propto f_{1,2}^2$: i.e. highly distorted and highly spinning neutron stars are the best sources.

The corresponding energies are not difficult to calculate and will depend on a further time derivative of the mass quadrupole

$$\frac{dE_{\text{GW}}}{dt} = \frac{1}{5} \left\langle \frac{d^3 \mathcal{I}_{\bar{j}\bar{k}}}{dt^3} \frac{d^3 \mathcal{I}_{\bar{j}\bar{k}}}{dt^3} \right\rangle_2 \quad (27)$$

yielding in this case

$$\left(\frac{dE_{\text{GW}}}{dt} \right)_1 = \frac{8}{5} (2\pi f_1)^6 (\theta_w \varepsilon_p I)^2 = \frac{3}{4} (\pi f_1 r)^2 h_{c1}^2, \quad (28)$$

$$\left(\frac{dE_{\text{GW}}}{dt} \right)_2 = \frac{32}{5} (\pi f_2)^6 (\varepsilon_p I)^2 = \frac{3}{4} (\pi f_2 r)^2 h_{c2}^2. \quad (29)$$

3 Rotating Neutron Stars Deformed by Crystalline or Magnetic Stresses

The shear stress tensor T_{jk}^S of the stellar parts that are in a crystalline form (i.e. the crust) is the only force (together with the magnetic ones) that can prevent the star to be axisymmetric about its rotation axis: i.e. that can produce a wobble angle θ_w and an equatorial oblateness ε_e . In neutron stars the competition with the other forces is very difficult since the Coulomb interaction which is the source of T_{jk}^S is much weaker than the degeneracy effects and the nuclear interaction which are the sources of the isotropic pressure force p , and also far weaker than the gravitational interaction and centrifugal forces (the latter responsible for ε_p).

In what follows we will make some qualitative estimates of this. In general, in a stable

neutron star

$$F_{\text{grav}} \sim F_{\text{press}} \sim \frac{M}{R^2} \rho \sim \frac{p}{R}, \quad (30)$$

and when the star is rotating additional centrifugal forces appear

$$F_{\text{cent}} \sim \Omega_{\text{rot}}^2 R \rho \lesssim F_{\text{grav}}. \quad (31)$$

which contrast the first two and give rise to the spheroidal oblateness

$$\varepsilon_{\text{p}} \sim \frac{F_{\text{cent}}}{F_{\text{grav}}} \sim \frac{(\Omega_{\text{rot}} R)^2}{M/R} \sim \left(\frac{0.5 \text{ msec}}{P_{\text{rot}}} \right)^2 \sim 10^{-2} - 10^{-4}. \quad (32)$$

3.1 Crystalline Stresses

Let us now compare this with the shear stresses induced by the crust and that are given by the standard stress-strain relation $T_{jk}^S = -2\mu\sigma_{jk}$, where μ is the *shear modulus* and σ_{jk} the dimensionless shear strain. Note that σ_{jk} is basically the deformation of the crystal from

the shape it would have in the absence of shear forces, i.e. its “reference shape”. Clearly, we want to consider those stars that differ most from their reference shape as these are going to be the strongest emitters.

In this case, $\sigma_{jk} \sim \sigma_{\text{break}}$, i.e. the deformation will be near break-up and the shear force will then be

$$F_{\text{shear}} \sim \frac{T_{jk}^{\text{S}}}{R} \sim \frac{\mu \sigma_{\text{break}}}{R} \lesssim F_{\text{cent}}, \quad (33)$$

producing a deformation of the shear-free, non-radiating shape that is

$$(\varepsilon_{\text{e}})_{\text{shear}} \sim \theta_{\text{w}} \varepsilon_{\text{p}} \sim \frac{I_{\text{c}} F_{\text{shear}}}{I F_{\text{grav}}} \sim \frac{I_{\text{c}} \mu \sigma_{\text{break}}}{I \rho M/R}. \quad (34)$$

Here $I_{\text{c}} \simeq 10^{-3} I$ is the crust’s contribution to the moment of inertia I and both μ and the density are those in the crust, i.e. $\rho \sim 10^{12} \text{ gr cm}^{-3}$. Unfortunately, all of these quantities are not well known and vary sensitively on the equation of state used or on the temperature

of the neutron star. In general, however, the present expectation is that $(\varepsilon_e)_{\text{shear}}$ and thus $\theta_w \varepsilon_p$ produced by shear stresses are *unlikely to exceed* 10^{-4} in any neutron star.

3.2 Magnetic Stresses

Crystalline stresses are not the only ones present in magnetized neutron star and, indeed, magnetic stresses in a pulsar might produce comparable deformations if the magnetic fields are sufficiently intense. In the highly conducting matter composing neutron stars, in fact, the magnetic field will introduce a magnetic pressure p_{mag} orthogonal to the field lines and a magnetic tension $-p_{\text{mag}}$ along the field lines.

Clearly, also in this case, precise estimates will depend on a number of details such as intensity of the magnetic field, its location, its lifetime, etc. However, on simple dimensional

arguments we can estimate that

$$F_{\text{mag}} \sim \frac{p_{\text{mag}}}{R} \sim \frac{B^2/8\pi}{R} \lesssim F_{\text{cent}}, \quad (35)$$

which will be responsible for a magnetically-induced equatorial oblateness

$$(\varepsilon_e)_{\text{mag}} \sim \theta_w \varepsilon_p \sim \frac{I_c F_{\text{mag}}}{I F_{\text{grav}}} \sim \frac{I_c p_{\text{mag}}}{I p} \sim 10^{-8} \left(\frac{B_{\text{crust}}}{10^{12} \text{ G}} \right)^2. \quad (36)$$

where B_{crust} is the magnetic field in the crust and which is expected to be close to the measured surface one of $\sim 10^{12}$ G.

4 Radio Pulsars

I have shown how the wave amplitude will depend quadratically on the rotation frequency and given the present limits of gravitational wave detectors, it is clear that there is a limit frequency $f_{\min} \sim 10$ Hz below which the pulsar will be invisible. Fortunately, there are two known and well studied populations of neutron stars that are observed to spin at frequency larger than f_{\min} : *fast, young* radio pulsars and *old, recycled* radio pulsars. Hereafter we will concentrate on the first ones only.

Fast and young radio pulsars spin down as a consequence of the emission of electromagnetic radiation produced by the rotation of the intense magnetic dipole. The rate of change of the period is extremely small, $P_{\text{rot}} \dot{P}_{\text{rot}} \simeq 10^{-15} B_{12}^2$ sec, ie less than a second over 100 million years, thus making these the best clocks in the Universe.

If the emission of electromagnetic radiation is dominant over the gravitational one (e.g. because of very intense magnetic fields), the rotation period will evolve as

$$P_{\text{rot}}^2 = P_i^2 + (10 \text{ msec})^2 \left(\frac{B}{4 \times 10^{12} \text{ G}} \right)^2 \left(\frac{\tau}{100 \text{ years}} \right). \quad (37)$$

If, on the other hand, the emission of gravitational radiation is dominant (e.g. because the magnetic field has decayed but the rotation is still very large²), the rate of change in the period will be $P_{\text{rot}}^3 \dot{P}_{\text{rot}} \simeq 3 \times 10^{-11} \varepsilon_e^2 \text{ sec}^3$ and the rotation period itself will evolve as

$$P_{\text{rot}}^4 = P_i^4 + (2.4 \text{ msec})^4 \left(\frac{\varepsilon_e}{10^{-6}} \right)^2 \left(\frac{\tau}{10^4 \text{ years}} \right). \quad (38)$$

In this case, the characteristic amplitudes that are expected in the most favourable conditions are

$$\left[\left(h_{c2}^2 + \frac{1}{4} h_{c1}^2 \right)^{1/2} \right]_{\text{max}} = \frac{1}{r} \left(\frac{4I \dot{P}_{\text{rot}}}{3 P_{\text{rot}}} \right)^{1/2} \simeq 3 \times 10^{-25} \left(\frac{10 \text{ kpc}}{r} \right) \left(\frac{10^3 \text{ years}}{P_{\text{rot}}/\dot{P}_{\text{rot}}} \right)^{1/2}. \quad (39)$$

²If Ohmic decay is effective in young neutron stars, the magnetic field will decay with an e-folding time of $\sim 10^7$ years.

One well-known example of fast and young pulsar is PSR 0531+21 which has $P_{\text{rot}} = 33\text{ms}$ corresponding to a gravitational wave frequency $f_2 = 60\text{ Hz}$. Also known as the “*Crab pulsar*” because it resides in the Crab nebula at $r \sim 2\text{ kpc}$ from us, this pulsar is about 1000 years old. Partially because it is much better known than others, at the moment the Crab pulsar is one of the most promising sources of gravitational waves and potentially observable by advanced interferometers over long-term (i.e. $\sim 1\text{ year}$) observations.

5 Oscillating Neutron Stars

The issue of the *detectability* of the gravitational radiation from perturbed relativistic stars is still basically unsettled. This is largely due to our ignorance about the precise physical conditions leading to a perturbed relativistic star. A simple example in this sense is offered by a protoneutron star formed after the gravitational collapse in a supernova explosion. While it is generally expected that the newly born neutron star will pulsate wildly during the first few seconds following the collapse, how much energy will be transferred to the pulsation and subsequently radiated through the oscillation modes is unknown. The only realistic way of overcoming this ignorance is to perform detailed, fully relativistic simulations and deduce from them how large the perturbations will be. While the recently developed numerical codes will soon be able to provide some quantitative answer in this

respect, at present one can simply argue that *a)* the energy stored in the pulsation can potentially be of the same order as the kinetic energy of the system; *b)* the oscillations will be damped mainly through the emission of gravitational waves so that the released energy could be considerable.

Under these assumptions, the effective gravitational wave amplitude h for a star oscillating in its fundamental mode of oscillation can be estimated simply. For weak gravitational waves, in fact, the gravitational wave luminosity (i.e. the rate of energy loss to gravitational waves) at a distance r , can be written to be [9]

$$\frac{dE}{dt} \simeq \frac{E}{\tau} \simeq 4\pi r^2 \left(\frac{c^3}{16\pi G} \right) |\dot{h}|^2, \quad (40)$$

where E is the total energy lost over the time τ . If the star is oscillating at a frequency f ,

then $\dot{h} \approx 2\pi fh$ and expression (40) can be rewritten as

$$h \simeq 1.2 \times 10^{-21} \left(\frac{E}{\tilde{E}} \right)^{1/2} \left(\frac{1 \text{ ms}}{\tau} \right)^{1/2} \left(\frac{1 \text{ kHz}}{f} \right) \left(\frac{50 \text{ kpc}}{r} \right), \quad (41)$$

where $\tilde{E} = 8.2 \times 10^{-8} M_{\odot} c^2$ is the energy lost in gravitational waves as estimated through recent relativistic calculations [10]. Note that the probability of detecting a source can be increased if suitable data analysis techniques, such as “matched filtering”, are used [11, 12].

In this case, it is possible to estimate the “effective” gravitational wave amplitude h_{eff} to be $h_{\text{eff}} \simeq h\sqrt{f\tau}$, so that (41) becomes

$$h_{\text{eff}} \simeq 1.2 \times 10^{-21} \left(\frac{E}{\tilde{E}} \right)^{1/2} \left(\frac{1 \text{ kHz}}{f} \right)^{1/2} \left(\frac{50 \text{ kpc}}{r} \right). \quad (42)$$

The distance scale r used in expressions (41) and (42) is that to the supernova SN1987A and the number of events in the corresponding volume is one every 10–20 years. Clearly, this event rate is too small for being of interest and it is therefore necessary to consider a

volume much larger, such as the one comprising the Virgo cluster, to reach an event rate of a few per year. In this case, it is possible to consider the problem of the detection from a different point of view and rather calculate the energy E necessary to obtain an effective wave amplitude $h_{\text{eff}} \sim 10^{-21}$ for a source at a distance $r = 20$ Mpc. Using expression (42), the answer is $E \approx 0.01 M_{\odot}$. While these estimates may appear optimistic of at least a couple of orders of magnitude, they cannot be ruled out and the pay-offs of a potential detection would be so great to justify the intense research this field is experiencing.

6 Non-axisymmetric Instabilities

Some of the non-axisymmetric modes of oscillation in rotating stars may not be damped, but have amplitudes that grow exponentially in time. When this is the case, the oscillations are said to be "unstable" and the resulting instability can either be *dynamical*, if it develops on the timescale set by the rotation or by the free-fall, or *secular*, if it develops on a much longer timescale set, for instance, by dissipative processes. Dynamical instabilities differ considerably from secular ones in that they are purely hydrodynamical, while the latter are triggered by dissipative processes such as viscous dissipation, emission of gravitational or electromagnetic radiation, thermal losses, etc.. In both cases, however, the instabilities reflect the attempt of the rotating star to find a lower energy state either by changing its mass distribution (e.g. through variations of the momentum of inertia) or by violating the con-

servation of some quantity (e.g. circulation or angular momentum). A quantity which is often used to measure how close the rotating star is to the onset of an instability is the so called *rotational parameter* β

$$\beta \equiv \frac{\text{(rotational kinetic energy)}}{\text{(gravitational energy)}} \equiv \frac{T}{|W|} \approx \frac{1}{3} \left(\frac{\Omega}{\Omega_K} \right)^2, \quad (43)$$

The last equality in (43) has been derived for a Newtonian star, with Ω/Ω_K being the stellar angular velocity normalized to the Keplerian value, that is, the value of the angular velocity at which matter can be shed at the stellar equator. Indicating with $\bar{\rho}$ the average rest-mass density, the Keplerian angular velocity can be estimated to be $\Omega_K \sim (2/3)\sqrt{\pi\bar{\rho}}$.

The parametrization (43) is independent of the rotation law and is particularly useful for differentially rotating objects. By definition and invoking the Virial theorem, the parametrization is constrained to be between $\beta = 0$ (for a spherical object) and $\beta = 1/2$ (for

an infinitely extended, thin disc at rest) [5]. A well-known application of the rotational parameter (43) is offered by classical result for the onset of the dynamical instability in Newtonian rotating stars, and which has been estimated to be $T/|W| \simeq 0.27$ for a variety of different equations of state and rotation laws.

Since the secular non-axisymmetric instabilities are triggered by dissipative mechanisms, their development will be different according to whether they are driven by viscous processes or by the emission of radiation (either gravitational or electromagnetic). When viscous dissipation processes are present and the radiative losses are negligible, an initially axisymmetric, incompressible rotating object, i.e. a *Maclaurin spheroid*, will be deformed into a *Jacobi ellipsoid*, i.e. into a uniformly rotating, homogeneous configuration with ellipsoidal surfaces (they are similar to rotating american “footballs”). This happens at roughly $T/|W| \simeq 0.14$ and is referred to as the viscous-driven f -mode instability (see [6] for a com-

plete discussion).

When viscous processes are negligible, on the other hand, the growth of the non-axisymmetric modes can be driven by the emission of gravitational or electromagnetic radiation (although the latter is usually much smaller than the former). The instability that develops in this way is the so called CFS (Chandrasekhar-Friedman-Schutz) instability [7, 8] and is produced by the coupling between the loss of energy and angular momentum via radiation and the non-axisymmetric oscillations modified by the stellar rotation. Also in this case, an initially axisymmetric Maclaurin spheroid will be deformed into a uniformly rotating, homogeneous configuration with ellipsoidal surfaces, called *Dedekind ellipsoid*. The difference between the Jacobi and Dedekind ellipsoids is that in the latter the ellipsoidal surfaces are supported by internal circulations but the shape is stationary as observed by an inertial observer (they are therefore similar to nonrotating american “footballs”). This

happens again at roughly $T/|W| \simeq 0.14$ and is referred to as the f -mode CFS-instability.

In practice, the development of non-axisymmetric instabilities is much more complicated than what discussed in the two limiting cases above, because *both* viscous and radiative losses are active at the same time in realistic stars. As a result, the modes that are driven unstable by viscosity and deform a Maclaurin spheroid into a Jacobi ellipsoid (i.e. the Jacobi modes) tend to be stabilized by the emission of gravitational waves (the star develops non-axisymmetric “ripples” to remove the excessive angular momentum via the emission of gravitational waves). At the same time, the modes that are driven unstable by the emission of gravitational waves and deform a Maclaurin spheroid into a Dedekind ellipsoid (i.e. the “Dedekind modes”) tend to be stabilized by the viscous dissipative processes (the increased shear stresses, for example, tend to remove, with the aid of the shear viscosity, the non-axisymmetric “ripples” responsible for the emission of

gravitational waves). Computing the delicate balance between these two mechanisms in regimes of strong gravitational fields, high-density matter and temperatures is extremely difficult and at the core of the present research on the emission of gravitational waves from instabilities in relativistic stars.

Because of the very large amplitudes that the oscillation modes can reach when driven unstable, the amount of gravitational radiation emitted can become considerable and these unstable stars can then become promising sources of gravitational waves, potentially detectable by the gravitational-wave observatories now working or being under construction.

6.1 An Introduction to the CFS Instability

The instability was first discovered by Chandrasekhar [7], and subsequently considered by Friedman and Schutz [8], who have shown its generic nature. While a formal proof of the criteria for the instability are rather involved [8], qualitative arguments on the properties of the instability can be given simply using a couple of illustrative examples.

Consider, therefore, a rotating star which is undergoing non-axisymmetric oscillations. For simplicity I will consider the simplest non-axisymmetric perturbation with mode numbers $\ell = m = 2$. Because the star is rotating, the properties of the perturbations can be considered both in a reference frame which is corotating with it (i.e. the “rotating” frame) or in a reference frame which is not rotating and is fixed with respect to, say, distant stars (i.e. the “inertial” frame).

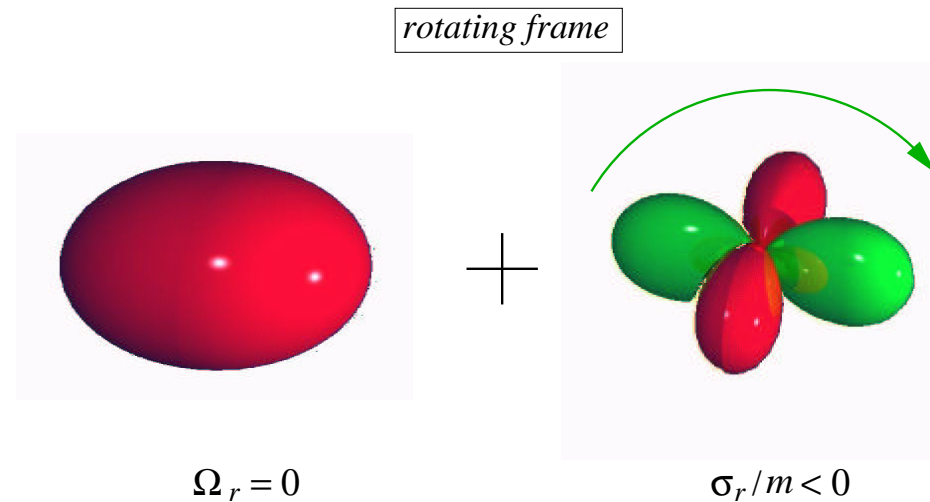


Figure 2: Schematic view from the rotating frame. The unperturbed star is shown on the left and the non-axisymmetric perturbation on the right. $\Omega_r = 0$ and σ_r/m are the angular velocities of the star and of the wave-pattern, respectively.

I will first discuss what would be observed in the rotating frame; this is summarized in Fig. 2 where I have shown schematically the unperturbed star on the left and the non-axisymmetric $\ell = m = 2$ perturbation on the right. In the corotating frame the star has a zero angular velocity (i.e. $\Omega_r = 0$), but is nevertheless deformed into a spheroid by the

centrifugal force. The perturbation on the other hand, has a nonzero frequency σ_r and the corresponding $m = 2$ wave-pattern is seen to rotate with angular frequency σ_r/m which is, say, negative. By definition, such a mode is referred to as “*retrograde*” and, because the perturbed star is rotating at an angular velocity smaller than the initial one, the mode has a *negative* angular momentum $J_0 < 0$ in the corotating frame.

The non-axisymmetric perturbation generates a time-variation of the stellar mass multipoles (and/or of the mass-current multipoles) and the gravitational waves that are produced in this way, carry positive amounts energy at infinity. The angular momentum carried at infinity j_{GW} , on the other hand, can either be positive or negative according to the sense in which the perturbation is seen to rotate in the inertial frame. I therefore need to consider how the perturbation is observed in the inertial frame which, I recall, is the frame in which quantities like the total amount of energy and angular momentum can be

measured unambiguously.

The “view” from the inertial frame is summarised in Fig. 3 where, again, I have shown schematically the unperturbed star on the left and the non-axisymmetric perturbation on the right. An observer in this frame will then see the star rotating at a nonzero, say positive, angular velocity $\Omega_i > 0$ and the non-axisymmetric perturbation with a wave pattern that is also rotating with angular velocity σ_i/m .

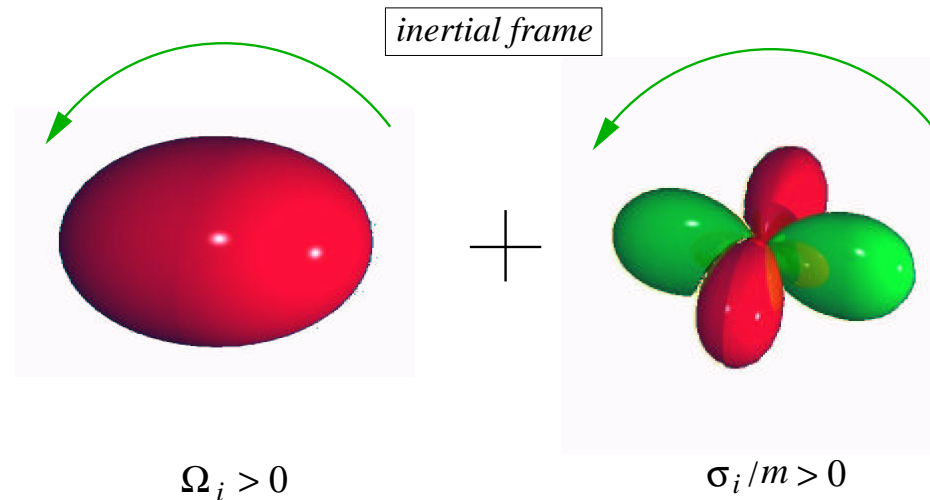


Figure 3: Schematic view from the inertial frame. The unperturbed star is shown on the left and the non-axisymmetric perturbation on the right. Ω_i and σ_i/m are the angular velocities of the star and of the wave-pattern, respectively.

It is not difficult to realize that the direction in which the wave-pattern rotates depends on both Ω_i and σ_r through the relation between the frequencies in the two reference frames: $\sigma_i = m\Omega_i - \sigma_r$. As a result, the wave-pattern can either be “dragged” forward ($\sigma_i > 0 > \sigma_r$), or backward ($\sigma_i < \sigma_r < 0$) by the stellar rotation Ω_i . The obviously interesting case shown

in Fig. 3, is the one in which the mode is dragged forward (i.e. $\sigma_i/m > 0$) and the non-axisymmetric mode, which is then said to be “*prograde*”, is seen to rotate in the same sense as the rotating star (Note that the “dragging” of the wave-pattern is a purely kinematical and Newtonian effect, fundamentally distinct from the general relativistic “dragging of reference frames”). When this happens, $\Omega_i\sigma_r < 0$ and the conditions for the onset of the CFS instability are met. In this case, in fact and, because the sign of the angular momentum lost is determined by the sense of rotation of the oscillation’s wave-pattern, the prograde non-axisymmetric perturbation will carry to infinity *positive* amounts of angular momentum, i.e. $j_{\text{GW}} > 0$.

For the observer in the rotating frame, on the other hand, the total angular momentum of the mode $J(t) \equiv J_0 - j_{\text{GW}}(t)$ becomes increasingly negative because of the losses through $j_{\text{GW}}(t)$ that continuously reduce $J(t)$, i.e. $J(t) < J_0 < 0$. As a result, the initially small non-

axisymmetric perturbation with negative angular momentum in the corotating frame, is driven to large amplitude oscillations with a progressively larger negative angular momentum. Such perturbation emits increasingly large amounts of gravitational waves, thus feeding the development of the instability. Using a pictorial analogue, the development of the CFS is similar to someone's debts that get larger as new expenses (with positive amounts of money) are made. The growth of the instability stops when either nonlinear or dissipative effects become important and transfer energy from the unstable mode into the other available channels.

References

- [1] C. W. Misner, K. S. Thorne and J. A. Wheeler, "*Gravitation*", Freeman, NY (1974)
- [2] B. F. Schutz, "*An Introduction to General Relativity*", Cambridge Univ. Press, Cambridge UK (1984)
- [3] R. d'Inverno, "*Introducing Einstein's Relativity*", Oxford Univ. Press, Oxford UK (1990)
- [4] S. Chandrasekhar, "*The Mathematical Theory of Black Holes*", Oxford Univ. Press, Oxford UK (1992)
- [5] Tassoul, "*Theory of Rotating Stars*", Princeton Univ. Press, Princeton (1978)
- [6] S. L. Shapiro and S. A. Teukolsky, "*Black Holes, White Dwarfs and Neutron Stars*", J. Wiley NY (1984)
- [7] S. Chandrasekhar, Phys. Rev. Letters **24**, 611 (1970)
- [8] J. L. Friedman and B. F. Schutz, Astrophys. Journ., **221**, 937 (1978); **222**, 281 (1978)
- [9] B. F. Schutz *Detection of gravitational waves* in Proceedings of "Astrophysical sources of gravitational radiation", J.A. Marck and J.P. Lasota Eds., Cambridge Univ. Press (1996)

- [10] H. Dimmelmeier, J. A. Font and Ewald Müller, *A&A* **393** 523; **388** 917 (2002)
- [11] C. Cutler and K. S. Thorne, *Proceedings of the GR16 Meeting*, N. T. Bishop and S. D. Maharaj Eds., World Scientific (2002)
- [12] S. A. Hughes, *Annals of Physics*, *in press*, astro-ph/0210481 (2002)
- [13] K. S. Thorne, *Lecture Notes Caltech*, Pasadena (1988)